Electronic Supplementary Information

One-reactor vacuum and plasma synthesis of transparent conducting oxide nanotubes and nanotrees: from single wire conductivity to ultra-broadband perfect absorbers in the NIR

Javier Castillo-Seoane,[1,2] Jorge Gil-Rostra,[1]* Victor López-Flores,[1] Gabriel Lozano,[3] F. Javier Ferrer,[4] Juan P. Espinós,[1] Kostya (Ken) Ostrikov,[5,6] Francisco Yubero,[1] Agustín R. González-Elipe,[1] Ángel Barranco,[1] Juan R. Sánchez-Valencia,[1,2] Ana Borrás[1]*

1) Nanotechnology on Surfaces and Plasma Group, Materials Science Institute of Seville, Consejo Superior de Investigaciones Científicas - Universidad de Sevilla, c/ Américo Vespucio 49, 41092, Sevilla, Spain

2) Departamento de Física Atómica, Molecular y Nuclear, Universidad de Sevilla, Avda. Reina Mercedes, E-41012, Seville, Spain

3) Multifunctional Optical Materials Group, Materials Science Institute of Seville, Consejo Superior de Investigaciones Científicas – Universidad de Sevilla (CSIC-US), c/ Américo Vespucio 49, Sevilla, 41092, Spain

4) Centro Nacional de Aceleradores (U. Sevilla, J. Andalucía, CSIC), Av. Tomás Alva Edison 7, Seville, 41092, Spain

5) School of Chemistry and Physics, Queensland University of Technology, Brisbane, QLD 4000, Australia.

6) CSIRO-QUT Joint Sustainable Processes and Devices Laboratory, Lindfield NSW 2070, Australia.

E-mail: jorge.gil@icmse.csic.es, anaisabel.borras@icmse.csic.es

Schematic S1. Scheme of the step-by-step formation of the ITO nanotubes (a) and nanotrees (b).

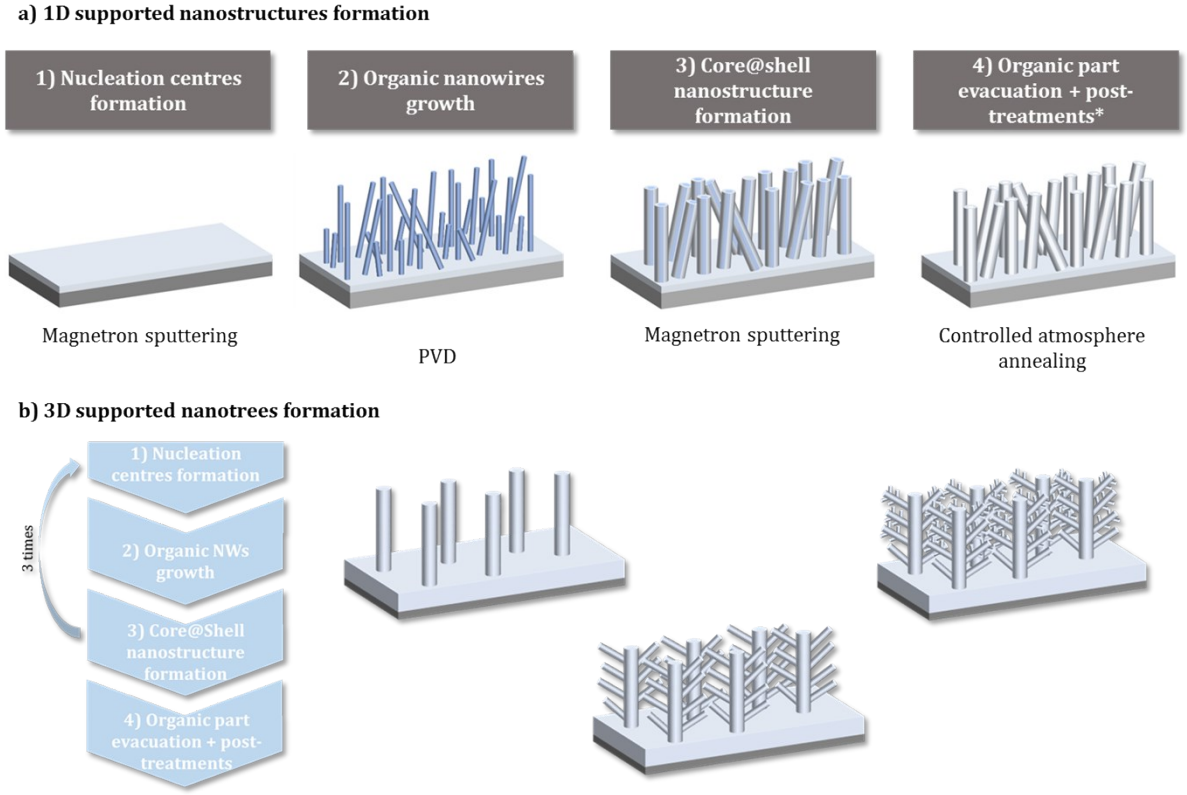

Step i) The seed or nucleation layer was deposited under "Low Pressure" conditions with a thickness of 120 nm.

Step ii) The fabrication of the single-crystalline ONWs is carried out by PVD in the following conditions: The H_2PC is evaporated in the Knudsen cell starting on its powder (provider details). In this step, the Ar flux was reduced to 10 cm^3/min and the substrate holder was cooled to 210 ºC (temperature determined in previous studies to get the best condensation – sublimation ratio of the molecules on the substrate surface that allows a fine nanowires growth),[1] the pressure was set at $1.0 \cdot 10^{-3}$ mbar and the Knudsen cell where was kept the organic compound powder is heated up sequentially until its sublimation temperature (~330 ºC). In order to get a slow deposition rate at the beginning to produce the nanowires nucleation centres, it was established Knudsen cell temperature increments which were 5 ºC in 5 minute intervals, starting at 0.03 Å/s. When the deposition rate became ~25.0 Å/s (microbalance control), it was only necessary to increase the temperature to keep this value approximately constant to get a homogeneous nanowires growth.

Step iii) Formation of the ITO shell by magnetron sputtering. The ITO shells were deposited using the same magnetron sputtering configuration and conditions detailed in the previous paragraph, i.e. LP and HP. In this case, there was a variation at the beginning which was the initial substrate holder temperature (210 ºC). This temperature was kept constant in the first deposition period (until a 1 KÅ thickness controlled by microbalance) to avoid the damaging of the organic core acting as template with sublimation temperatures close to 350 ºC. Once the initial layers of the ITO shell are deposited, the substrate temperature is heated up until the according temperature. This same strategy was settled in a previous article[2] to develop TiO_2 anatase nanotubes.

Step iv) The complete removal of the organic molecules was carried out by annealing in air atmosphere at 350ºC (heating ramp 2ºC/min) for 3 h and the cool down to RT (cooling ramp

5ºC/min). As final proof of concept, we extended the soft template methodology towards the formation of ITO nanotrees (ITO_NTrees) (see Schematic S1 b). The deposition method and the conditions were the same than the ITO_NTs samples but the steps ii) and iii) were repeated three times to each substrate. Using this approach, a nanostructured material with a three-dimensional morphology (a main central nanotube with secondary branching nanotubes) is formed as it is presented in the results section. After the organic core removal, ITO_NTs and ITO_Nanotrees samples were annealed in the main synthesis chamber in an argon atmosphere under a pressure of $2.5 \cdot 10^{-3}$ mbar (Ar flux = 30 sccm) for 3 hours at a temperature of 350 ºC.

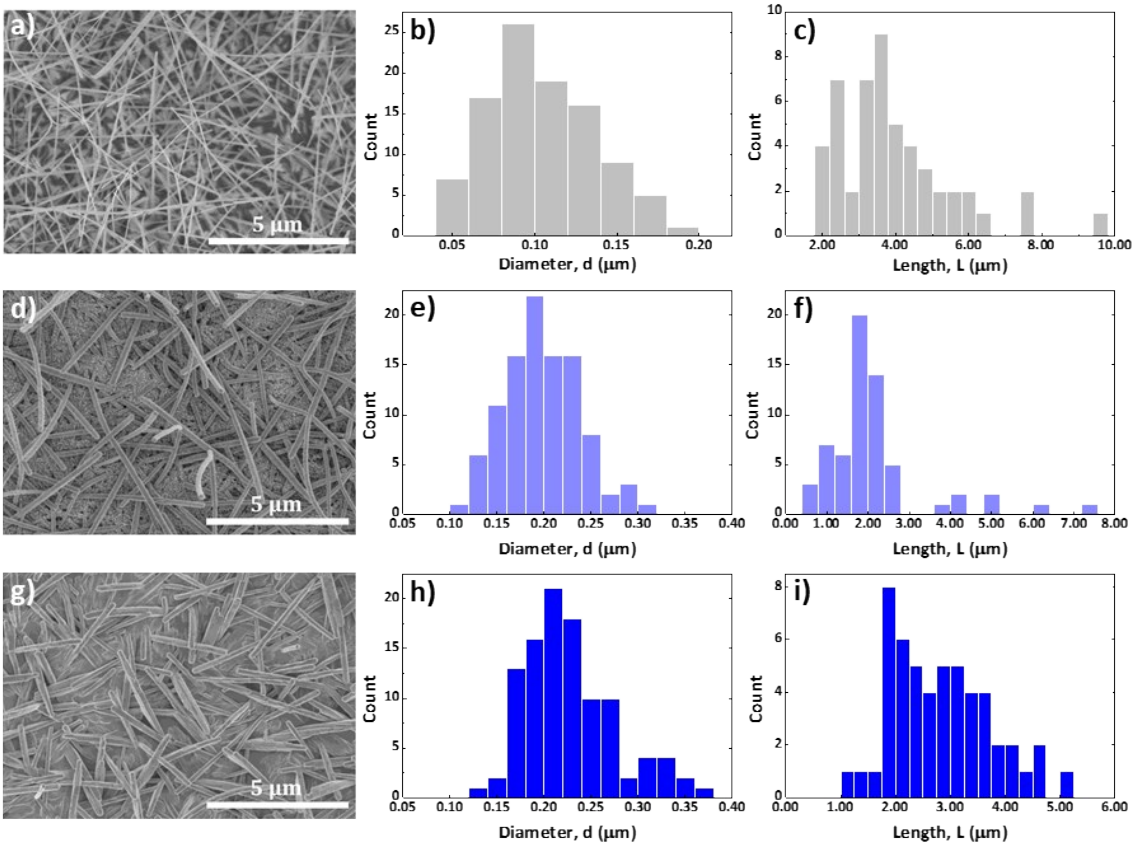

Figure S1. Statistical analysis of the ONWs (a, b), LP_NTs (c-d) and HP_NTs (e-f) length and thickness.

Table S1. Statistical SEM analysis results of ONWs and ITO nanotubes.

Sample/Measure	Diameter, D (µm)	Length, L (µm)	Density (n/µm²)
ONWs	0.10 ± 0.03	4.0 ± 1.6	6.5 ± 0.7
ITO NT -LP	0.19 ± 0.04	2.2 ± 1.2	2.7 ± 1.0
ITO NT -HP	0.22 ± 0.05	2.8 ± 0.9	3.3 ± 0.6

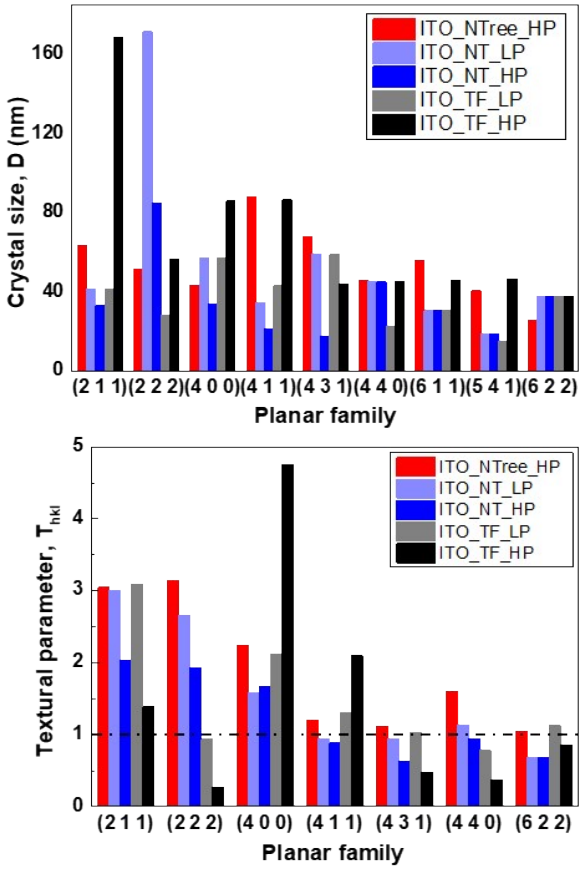

Figure S2. Crystal size (top) and textural parameter, T_{hkl} (bottom).

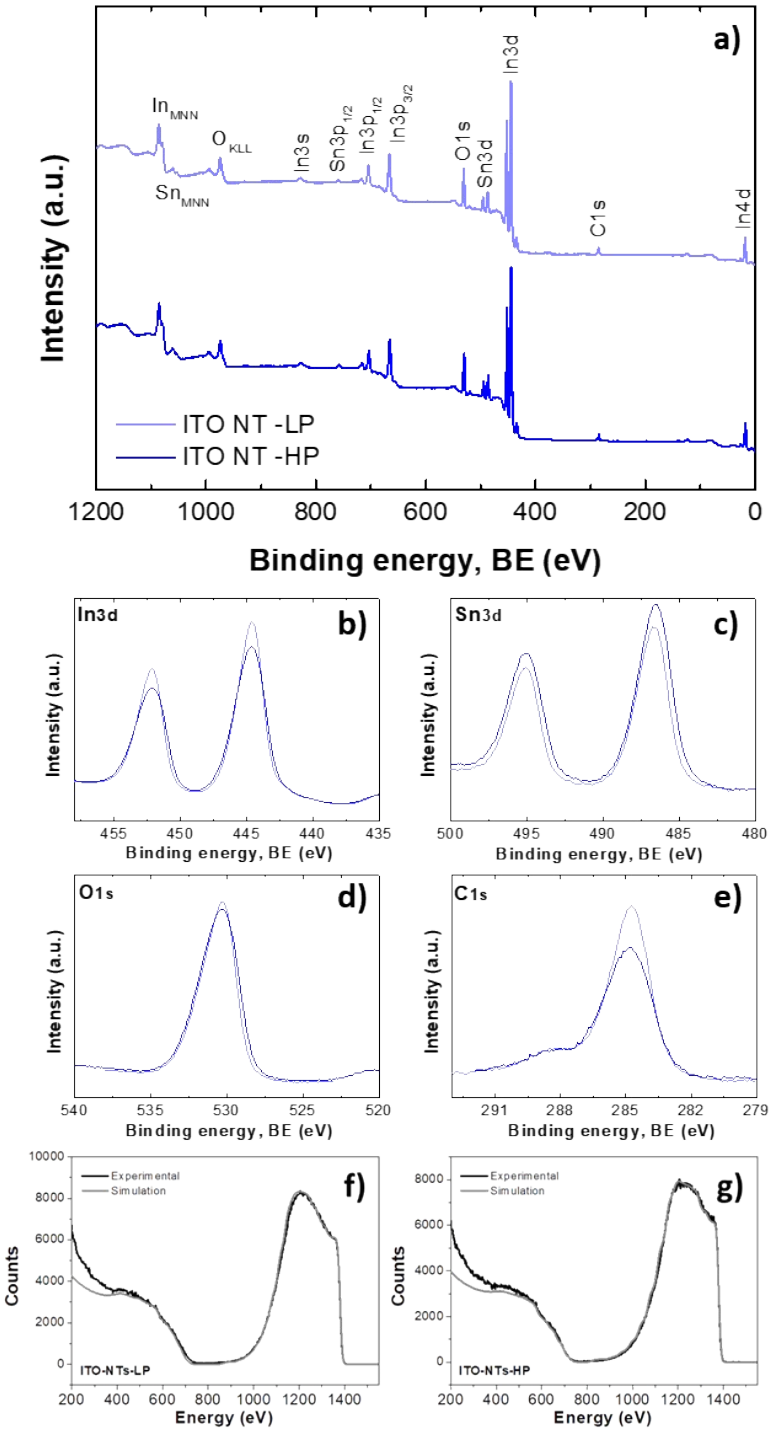

Figure S3. General (a) and peak (b-e) XPS spectra for the LP and HP ITO nanotubes; Experimental and simulated RBS spectra for LP (f) and HP (g) ITO nanotubes.

Table S2. XPS and RBS quantification results on the ITO nanotubes chemical composition after the post-treatment annealing.

XPS	**Sample/Peaks**		**C (1s) (at. %)**	**O (1s) (at. %)**	**In ($3d_{5/2}$) (at. %)**	**Sn ($3d_{5/2}$) (at. %)**	**Sn:(Sn+In)**
	ITO_NT_LP		19.2	41.7	35.1	4.0	0.10
	ITO_NT_HP		16.0	44.6	34.6	4.8	0.12
RBS	**Sample**		**Thickness (10^{15}at/cm^2)**	**[O] (at.%)**	**[In] (at.%)**	**[Sn] (at.%)**	**O:(In+Sn)**
	ITO_NT_LP	Substrate ↑	649 ± 23	61.8 ± 1.6	34.8 ± 1.5	3.4 ± 0.2	1.62 ± 0.11
		↓ NTs tips	680 ± 25	66.1 ± 1.5	31.0 ± 1.5	2.9 ± 0.2	1.94 ± 0.13
	ITO_NT_HP	Substrate ↑	748 ± 27	63.8 ± 1.5	33.0 ± 1.5	3.2 ± 0.2	1.76 ± 0.12
		↓ NTs tips	690 ± 26	65.9 ± 1.5	31.0 ± 1.5	3.0 ± 0.2	1.94 ± 0.13

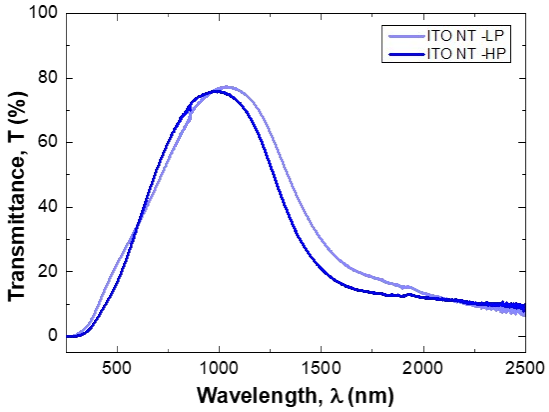

Figure S4. Comparison of direct transmittance spectra for the nanotube samples prepared on fused silica under low and high-pressure conditions.

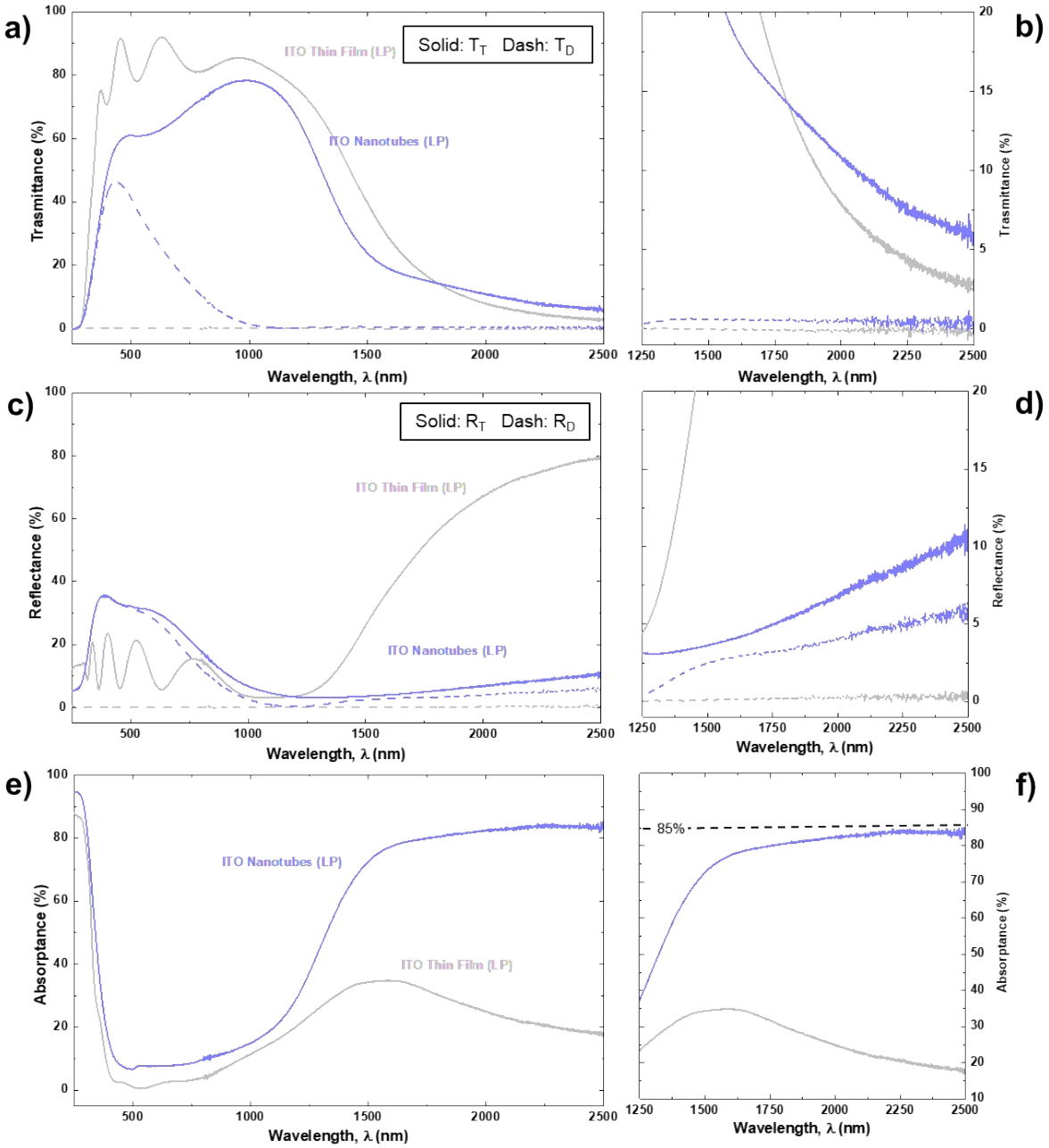

Figure S5. UV-vis-NIR spectra of ITO LP samples: (a) total and diffusive transmittance (T_T, T_D) and zoom-in in the NIR range (b); (c) total and diffusive reflectance (R_T, R_D) and zoom-in in the NIR range (d); (e) absorptance (e) and zoom-in in the NIR range (f).

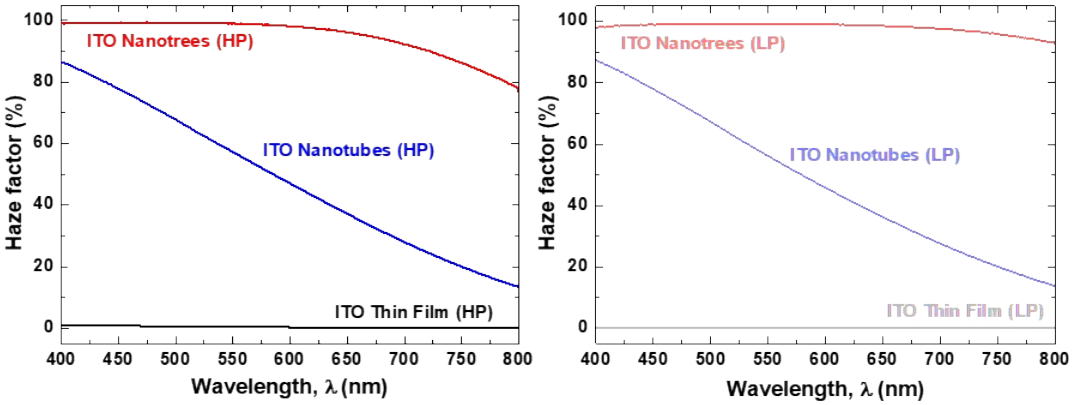

Figure S6. Comparison of the haze factors estimated for the three types of samples prepared under HP (left) and LP (right) conditions.

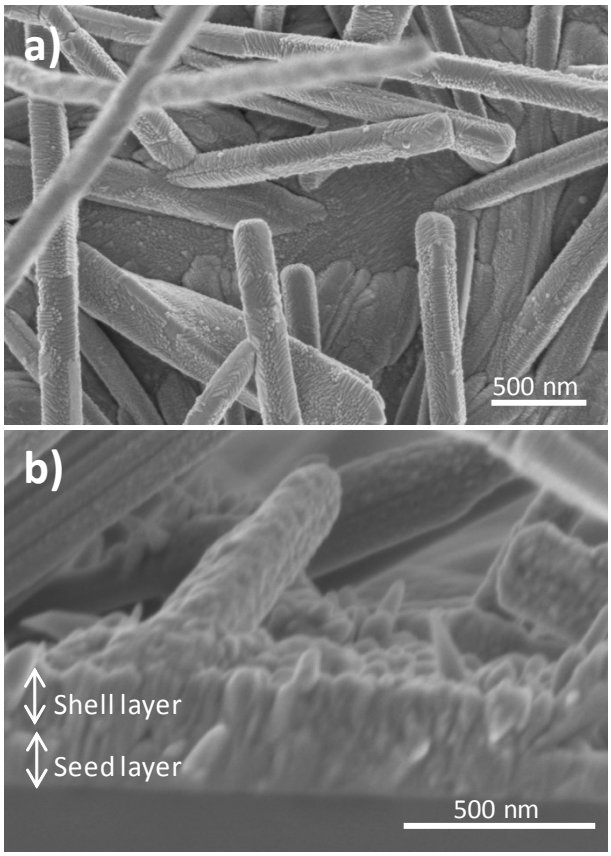

Figure S7. Normal view (a) and cross-section (b) SEM micrographs of an area with a low density of nanotubes showing the conformal growth of the shell layer on top of the seed layer.

Section S8.

The electrical characterization was carried out at two different levels aiming for both, macroscopic, thin films and nanotubes forming supported layers, and nanoscopic, i.e. individual nanotubes, scales. In both cases, the 4-point probe method was utilized. This methodology allows the characterization of thin films and nanostructures avoiding the problems associated with the contact resistance, R_c, with the electrodes. Thus,

this approach is often applied to circumvent the handicaps related to the electrical characterization of microstructured materials when the resistance in the contacts between wires and electrodes with the specimen is higher than the intrinsic to the specimen. In a typical experiment, the outer contacts are used to scan the current (I) in sweep mode while the voltage (V) induced between the other two probes is acquired.[3]

In the case of ohmic contacts with a conductive material, the obtained I-V curves usually fit to a straight line providing the estimation of the resistance (R_{sh}) by equation (ec.1).

$$R_{sh} = \pi\ ln2\ V\ I = \rho\ t \rightarrow \rho = R_{sh} \cdot t\ (ec.1)$$

Where R_{sh} is the sheet resistance, V the voltage, I the intensity, ρ the resistivity and t the thickness of the deposited material. However, to calculate the real sheet resistance of the film is necessary to apply several correction factors to take into account the finite sample dimensions.[3]

$$R_{sh} = F \cdot \pi \cdot ln2 \cdot V \cdot I\ (ec.2)$$

Three different factors for finite isotropic samples are discussed in the literature: $F=F_1 \cdot F_2 \cdot F_3$ (ec.3). F1 considers the effects of the finite thickness of the samples. For very thin samples t/s < 0.1, where t is the thickness of the sample and s is the separation of the electrodes (0.33 mm in our 4-point cell), this factor is one. F2 take into consideration the probes proximity of the sample edge. Our materials were deposited on fused silica substrates of 2.5x2.5 cm^2, so the extreme probes are separated at least 0.75 cm from the edge. The correction factor F2 can be considered as the unity too in this case. And the last correction factor, F3, is linked with the sample size. This factor is around 0.8 considering that the sample size is around 8 times bigger than the separation of the electrodes. Thus, the total correction factor is F=0.8. See additional details in reference.[3]

The macroscopic characterization was carried out in a four-probe cell made by the Nanotechnology on Surfaces research group equipped with a sourcemeter working in sweep voltage/current mode under ambient conditions (Figure S7 a)). The sourcemeter was a Keithley 2635A system with resolution in the range of 100 pA. Measurements were done for the thin film and nanotube layer samples deposited on fused silica substrates.

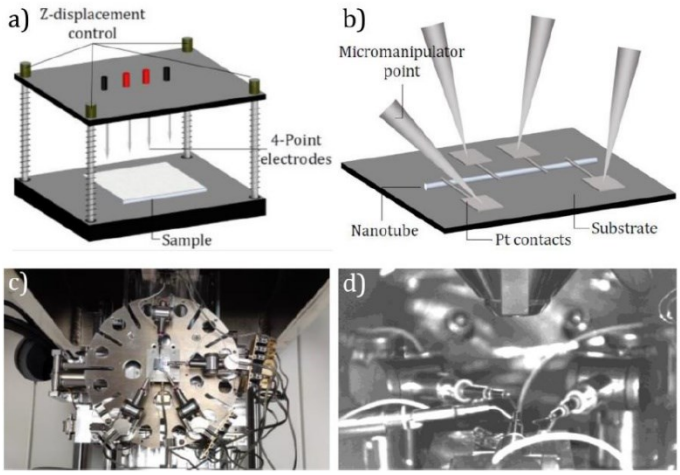

Figure S8. Schematics of a) a four-point probe cell and b) four-point probe method applied by micromanipulators on a nanotube; In both configurations, current flows between the two external electrodes while voltage is measured in the two central electrodes. Images of c) the top view of a micromanipulators stage and d) a general view of a micromanipulators stage into a SEM chamber.

The equivalent characterization for individual nanotubes requires additional processing of the samples to contact the NTs by micrometric electrodes. This step enables the four nanoprobe electrical measurements assisted by SEM.

The samples were characterized in a Zeiss Gemini SEM 300 equipped with 4 Kleindiek manipulators and nanoprobes (see Figure S7 c-d). Equation (ec.4) addresses the relationship between the resistance R obtained from the slope[4] of the I-V curves and the resistivity of the NTs characterized by this single-wire approach.

$$R = \rho \cdot L \cdot \pi \cdot (r_2^2 - r_1^2) \rightarrow \rho = R \cdot \pi \cdot (r_2^2 - r_1^2) \cdot L \ (ec.4)$$

Where L is the distance between the two central Pt contacts, r_1 the internal nanotube radius and r_2 the external nanotube radius.

References

1 A. Borras, P. Gröning, J. R. Sanchez-Valencia, A. Barranco, J. P. Espinos and A. R. Gonzalez-Elipe, *Langmuir*, 2010, **26**, 1487–1492.

2 A. N. Filippin, J. R. Sanchez-Valencia, J. Idígoras, T. C. Rojas, A. Barranco, J. A. Anta and A. Borras, *Nanoscale*, 2017, **9**, 8133–8141.

3 I. Miccoli, F. Edler, H. Pfnür and C. Tegenkamp, *J. Phys.: Condens. Matter*, 2015, **27**, 223201.

4 A. S. Walton, C. S. Allen, K. Critchley, M. \L Górzny, J. E. McKendry, R. M. D. Brydson, B. J. Hickey and S. D. Evans, *Nanotechnology*, 2007, **18**, 065204.